Geochemical Perspectives Letters

Comparative ^{142}Nd and ^{182}W study of MORBs and the 4.5 Gyr evolution of the upper mantle

D. Peters[1], H. Rizo[1*], J. O'Neil[2], C. Hamelin[3], S.B. Shirey[4]

OPEN ACCESS

https://doi.org/10.7185/geochemlet.2412

Abstract

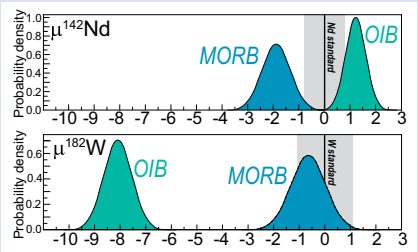

New high precision Nd and W isotopic compositions were obtained on the same basalt samples from the Pacific-Antarctic Ridge. These provide the best estimate so far for the μ^{142}Nd and μ^{182}W values of the depleted mantle source of mid-ocean ridge basalts known as DMM. The PAR basalts yield a mean $\mu^{142}Nd = -1.6 \pm 5.0$ (2 s.d.) and $\mu^{182}W = -1.9 \pm 3.5$ (2 s.d.), which together with the literature data allow the isotope composition of the DMM to be constrained. The present-day DMM μ^{182}W is 10–20 ppm lower than that of the Archean mantle. This decrease could be related to the broad incorporation of mantle plume material into the upper mantle, starting between 2.4 and 3 billion years ago, due to the onset of deep cold slab subduction, and its attendant return mantle flow.

Received 4 July 2023 | Accepted 28 February 2024 | Published 11 April 2024

Introduction

The Earth's mantle underwent significant chemical evolution during its early history. The short lived isotope systems ^{182}Hf-^{182}W ($t_{1/2} = 8.9$ Myr) and ^{146}Sm-^{142}Nd ($t_{1/2} = 103$ Myr) applied to the study of terrestrial rocks have provided valuable insights into understanding the nature of these changes, because they are especially capable of tracing the most ancient chemical fractionation processes. Notably, ancient mantle-derived rocks from various Archean cratons exhibit variations in ^{142}Nd abundances (*e.g.*, Carlson *et al.*, 2019), implying silicate differentiation within the first ~500 million years of Earth's history. The recent detection of ^{182}W abundance variations in mantle-derived rocks of different ages have initiated debates regarding the main processes controlling ^{182}W variability, including early silicate differentiation as seen by the ^{146}Sm-^{142}Nd system (*e.g.*, Touboul *et al.*, 2012), core-mantle chemical interactions (*e.g.*, Rizo *et al.*, 2019), differences in the mass of late accreted extra-terrestrial material into the mantle (*e.g.*, Willbold *et al.*, 2011) and the recycling of ancient crust or sediments into the mantle (*e.g.*, Tusch *et al.*, 2021).

Variations in ^{142}Nd and ^{182}W abundances, denoted as μ^{142}Nd and μ^{182}W, reflect part-per-million deviations from laboratory standards set at $\mu = 0$. These standards are assumed to represent the compositions of the modern mantle, or the depleted mid-ocean ridge mantle (DMM) reservoir. However, few mantle peridotites ($n = 4$), or melts directly derived from the depleted upper mantle such as MORB ($n = 9$), have been analysed for μ^{142}Nd (*e.g.*, Boyet and Carlson, 2006; Caro *et al.*, 2006; Cipriani *et al.*, 2011; Jackson and Carlson 2012; Hyung and Jacobsen, 2020). The W isotopic composition of the DMM has never been properly determined, given that only two MORB samples have been studied to date (Rizo *et al.*, 2016; Mundl *et al.*, 2017). Therefore, μ^{142}Nd and μ^{182}W of the upper mantle are presently inadequately constrained, yet are crucial for understanding the composition and chemical evolution of the silicate Earth.

This study presents new μ^{142}Nd data for fourteen MORB samples from the Pacific-Antarctic Ridge (PAR), therefore, tripling the current MORB dataset. We also report W concentrations for 18 samples, and μ^{182}W measurements for seven of these PAR samples. The studied MORB samples were collected between 53° S and 42° S (Fig. S-1), a fast-spreading ridge section with no nearby hotspots. All fresh MORB samples were collected on-axis, and have previously been thoroughly characterised for their petrology, geochemistry and isotopic compositions (*e.g.*, Sr, Nd, Pb, Hf, He, D, S, and Mo), showing the lack of plume influence (Hamelin *et al.*, 2011; see Supplementary Information for sample descriptions). The MORB μ^{142}Nd and μ^{182}W are used to provide the first robust estimate for the DMM supplying the Pacific-Antarctic Ridge.

The μ^{182}W and μ^{142}Nd of the Upper Mantle Sources Supplying the PAR Basalts

As mantle-derived melts devoid from continental crustal contamination, MORBs allow to constrain the μ^{142}Nd and μ^{182}W of the upper mantle. The low W abundance of MORB samples,

1. Department of Earth Sciences, Carleton University, 1125 Colonel By Drive, Ottawa, ON K1S 5B6, Canada
2. Department of Earth and Environmental Sciences, University of Ottawa, 150 Louis-Pasteur Private, Ottawa, ON K1N 6N5, Canada
3. Independent Scholar, Søndre Skogveien 7, 5055 Bergen, Norway
4. Earth and Planets Laboratory, Carnegie Institution for Science, 5241 Broad Branch Road NW, Washington DC, 20015, U.S.A.
* Corresponding author (email: hanika.rizo@carleton.ca)

however, makes them susceptible to disturbances related to element mobility or secondary hydrothermal alteration overprinting. This concern does not apply to the less mobile Nd, for which concentration in basalts is higher. Therefore, evaluating whether the W hosted in these rocks is of igneous origin is imperative.

Tungsten concentrations in the studied PAR MORBs ($n = 18$) vary from 6.8 ng g^{-1} to 220 ng g^{-1} (Data Table S-1) and are strongly coupled to other immobile and highly incompatible trace elements, such as Th and Nb (Fig. S-2a, b). Narrow ranges for W/Th = 0.1–0.15 (Fig. S-2d), W/Ba = 0.0019–0.0027, W/Ta = 0.08–0.16, and W/U = 0.23–0.43 (not shown) indicate that the W contained in the MORB samples is derived from their mantle sources and free from secondary hydrothermal W overprinting (*e.g.*, König *et al.*, 2011). Therefore, the W isotopic analyses of these samples accurately establish the $\mu^{182}W$ of their mantle sources.

The $\mu^{182}W$ of the PAR MORBs range from -3.9 ± 4.1 (2 s.e.) to 1.0 ± 2.9 (2 s.e.) with a mean of -1.9 ± 3.5 (2 s.d.; $n = 7$) (Table 1 and Fig. 1a; Method and detailed isotope data in the Supplementary Information). These results are undistinguishable within errors from the $\mu^{182}W$ values of -0.8 ± 4.5 (2 s.e.) and 3.5 ± 4.0 (2 s.e.) in MORBs, respectively, from the East Pacific Rise (Rizo *et al.*, 2016) and the Central Indian Ridge (Mundl *et al.*, 2017). The narrow W isotopic variability observed across three mid-ocean ridge segments from a sparse worldwide coverage suggests that there is little $\mu^{182}W$ variation outside the analytical uncertainties within the DMM, on a regional and global scale.

The PAR MORB $\mu^{142}Nd$ range from -5.7 ± 2.3 (2 s.e.) to 2.8 ± 2.4 (2 s.e.), with a mean of -1.6 ± 5.0 (2 s.d.; $n = 14$) (Fig. 1b). Eleven out of 14 samples show $\mu^{142}Nd$ within the uncertainty of the JNdi-1, and three samples exhibit lower $\mu^{142}Nd$ between -5.7 ± 2.3 (2 s.e.) and -5.0 ± 2.4 (2 s.e.). Most $\mu^{142}Nd$ of PAR MORB are within errors of basalts collected from five other ridges (Fig. 1b), showing little $\mu^{142}Nd$ variability outside the analytical precision of measurements, regionally or globally, consistent with the $\mu^{182}W$.

Hadean Differentiation Between DMM and OIB Sources?

MORB and abyssal peridotite samples are the best proxies for the $\mu^{142}Nd$ of the DMM. Although the $\mu^{142}Nd \leq -5$ values of some MORB and mantle peridotite samples are not resolvable from the $\mu^{142}Nd$ of standards (Fig. 1b), they suggest the presence of Hadean mantle heterogeneities in the DMM, given that ^{142}Nd variability can only be produced by Sm/Nd fractionation occurring before the extinction of ^{146}Sm (*i.e.* before ~4 Ga). Recent studies propose that Earth's building blocks may have been characterised by $\mu^{142}Nd$ of ~−7.5 (*e.g.*, Frossard *et al.*, 2022; Johnston *et al.*, 2022), and a $^{147}Sm/^{144}Nd$ ratio of ~0.201 — approximately 2.5 % higher than the chondritic reference value of 0.1960 (to evolve from initial $\mu^{142}Nd$ ~−7.5 to 0 today). Consequently, the low $\mu^{142}Nd$ values (≤−5) detected in certain MORB and mantle peridotite samples might be relics of these primordial components in the DMM. Preservation of primordial heterogeneities in the DMM is, however, difficult to explain. Not only must they survive the mixing of Earth's magma ocean stage, but must also evolve with a near-chondritic Sm/Nd ratio during the Hadean to preserve their $\mu^{142}Nd$ (≤−5) measured today. This early, near-chondritic Sm/Nd ratio contrasts with the later, superchondritic Sm/Nd ratio required to explain the $\varepsilon^{143}Nd > +8$ of all analysed PAR MORB samples, even including those exhibiting low $\mu^{142}Nd$.

Intriguingly, the weighted mean $\mu^{142}Nd$ of all available data for MORB and mantle peridotites ($\mu^{142}Nd = -1.6 \pm 0.9$; $n = 27$), and OIB ($\mu^{142}Nd = +2.0 \pm 0.6$; $n = 66$) (Fig. 2a) reveals slight differences, suggesting distinct mantle sources and evolutionary histories. Despite the small ^{142}Nd difference of ~3.6 ppm falling within the range of current analytical precision, a student's t-test comparing the datasets indicates a 99.99 % probability of significant difference (p-value of 9.45 x 10^{-5}). While t-tests are valid statistical methods for distinguishing datasets, they do not consider uncertainties associated with individual data points. To obtain the most accurate $\mu^{142}Nd$ estimates for the DMM and the OIB sources, Monte Carlo bootstrap simulations were

Table 1 $\mu^{182}W$ and $\mu^{142}Nd$ of MORBs from the Pacific-Antarctic Ridge. Detailed isotope compositions can be found in the Supplementary Information (Data Tables S-2 and S-3).

Sample	$\mu^{182}W$	± 2 s.e.	$\mu^{142}Nd$	± 2 s.e.
PAC2DR01-1	−1.7	3.2	−7.3	2.4
PAC2DR01-1 *duplicate 1*			−3.6	3.6
PAC2DR01-1 *duplicate 2*			−4.0	3.3
PAC2DR01-1 *average*			−5.0	2.4
PAC2DR02-1	1.0	2.9	0.2	2.5
PAC2DR04-2			−1.8	2.4
PAC2DR05-2g	−3.0	4.8	1.4	2.4
PAC2DR06-6	−1.1	3.5	0.5	1.6
PAC2DR08-1	−3.7	5.8	−2.8	2.2
PAC2DR20-1	−0.8	3.4	−1.0	2.4
PAC2DR22-1			−5.7	2.3
PAC2DR27-1	−3.9	4.1	−1.7	2.4
PAC2DR30-1			−0.04	3.2
PAC2DR31-3			2.8	2.4
PAC2DR32-1			−5.3	2.3
PAC2DR33-1			−1.8	2.4
PAC2DR36-1			−1.6	2.4
Mean ± 2 s.d.	*−1.9*	*3.5*	*−1.6*	*5.0*

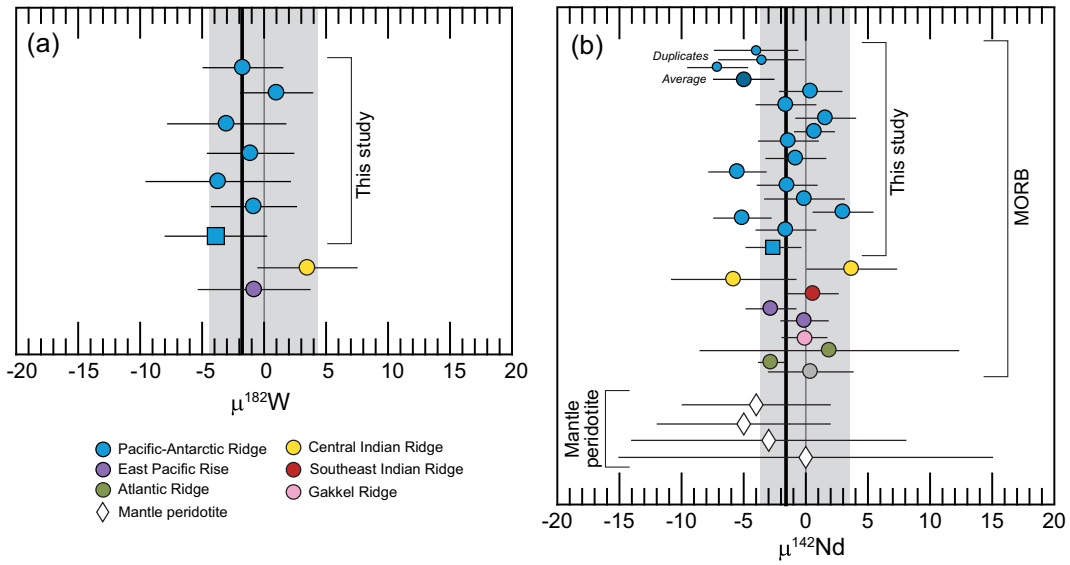

Figure 1 **(a)** $\mu^{182}W$ and **(b)** $\mu^{142}Nd$ for PAR MORBs of this study. Vertical thin grey lines with shaded areas show average standards ($\mu^{182}W = 0$ and $\mu^{142}Nd = 0$) with external reproducibility (2 s.d.). Vertical thick black lines show the mean for all MORBs analysed here ($\mu^{182}W = -1.9 \pm 3.5$; $\mu^{142}Nd = -1.6 \pm 5.0$). Smaller symbols in **(b)** are duplicate analyses with the average value and 2 s.d. in darker shade. MORB $\mu^{182}W$ of East Pacific Rise and Central Indian Ridge are, respectively, from Rizo *et al.* (2016) and Mundl *et al.* (2017). The $\mu^{142}Nd$ for other MORBs are from Boyet and Carlson (2006), Caro *et al.* (2006), Jackson and Carlson (2012), and Hyung and Jacobsen (2020), and mantle peridotite data from Cipriani *et al.* (2011).

conducted, accounting for uncertainties associated with each individual $\mu^{142}Nd$ data point. Figure 2b shows the resulting probability density plots, implying statistically distinguishable $\mu^{142}Nd$ values for the DMM and the OIB sources.

The lower average $\mu^{142}Nd$ value of the DMM compared to the OIB sources indicates differentiation before ~4 Ga. This early differentiation is consistent with the distinct $^{129}Xe/^{130}Xe$ ratios observed in MORB and OIB, also implying mantle differentiation around 4.45 Ga (Mukhopadhyay, 2012). Notably, a low Sm/Nd fractionation factor of ~0.02 at 4.45 Ga (defined as $^{147}Sm/^{144}Nd_{[newly\ formed\ reservoir]}/^{147}Sm/^{144}Nd_{[parent\ reservoir]} - 1$) can explain the observed ~3.6 ppm $\mu^{142}Nd$ difference between DMM and OIB sources. This scenario, however, requires the DMM to have evolved with a lower Sm/Nd ratio compared to the OIB sources, implying that the DMM was originally *less* depleted in incompatible elements compared to OIB sources. This contradicts the evidence that the DMM is *more* depleted, based on its present day $\varepsilon^{143}Nd$ of nearly +9 of MORB (Gale *et al.*, 2013). Oceanic crust sequestration and preferential slab subduction to the lower mantle have been proposed as a plausible model to deplete the lower mantle to a greater extent than the upper mantle (Tucker *et al.*, 2020). The seemingly opposite time-averaged Sm/Nd required to explain MORB $\mu^{142}Nd$ and $\varepsilon^{143}Nd$ requires Sm/Nd fractionation that could result from extraction of continental crust occurring after extinction of ^{146}Sm (after 4 Ga).

Modern Mantle $\mu^{182}W$ Heterogeneities – Established Early or Acquired Through Time?

A significant observation derived from our results is that the average $\mu^{182}W$ of the modern DMM (−1.9) is approximately 10 to 20 ppm lower than the average Hadean-Archean mantle (*e.g.*, Rizo *et al.*, 2019). This difference in $\mu^{182}W$ suggests the incorporation of a negative $\mu^{182}W$ component to the DMM, in order to decrease the $\mu^{182}W$ of the Archean mantle to the present day composition. Component candidates with negative $\mu^{182}W$ include: 1) an early-formed enriched crust or mantle domain, 2) late accretionary chondritic material, and 3) mantle plume material.

Negative $\mu^{182}W$ in the earliest oceanic crust, or differentiated mantle domain formed after Earth's magma ocean solidification, can result from Hf/W fractionation during the lifetime of ^{182}Hf (*i.e.* first ~50 Ma of Solar System history). The remixing of this negative $\mu^{182}W$ material into the mantle could lead to the observed decrease in $\mu^{182}W$ from the Archean to the modern mantle. If characterised by negative $\mu^{182}W$, such material would also exhibit negative $\mu^{142}Nd$. However, combined negative $\mu^{182}W$ and $\mu^{142}Nd$ have currently only been observed in ~3.6 Ga komatiites (Puchtel *et al.*, 2016). Although early mantle differentiation models capable of explaining decoupled ^{182}W and ^{142}Nd have been proposed (*e.g.*, Tusch *et al.*, 2022), these still require an initial ~4.35 Ga source with low $\mu^{182}W$ and low $\mu^{142}Nd$, which existence has yet to be proven. Furthermore, although some negative $\mu^{182}W$ has been detected in Paleoarchean rocks and diamictites from South Africa (Puchtel *et al.*, 2016; Mundl *et al.*, 2018; Tusch *et al.*, 2022), more than 95 % of ancient rocks currently analysed instead have positive $\mu^{182}W$ between +10 and +20 (*e.g.*, Rizo *et al.*, 2019). The scarce evidence for negative $\mu^{182}W$ in ancient rocks, and the rather constant positive $\mu^{182}W$ in throughout the Archean, suggests that if abundant negative-$\mu^{182}W$ material existed, either early crustal subduction was deep enough to escape subsequent sampling, or most of that negative $\mu^{182}W$ crust has now been recycled into the mantle.

Alternatively, the late accretion of materials with chondritic bulk compositions after core formation is a hypothesis proposed to account for the abundance of highly siderophile elements (HSE) in the upper mantle. This accretion could also explain the decrease of $\mu^{182}W$ of the DMM (*e.g.*, Willbold *et al.*, 2011), given the $\mu^{182}W$ of ~−200 of chondrites (*e.g.*, Kleine and Walker, 2017), and would be unrelated to $\mu^{142}Nd$. The common absence of correlations between $\mu^{182}W$ and HSE abundances (*e.g.*, Rizo *et al.*, 2019), however, suggests that late accretion is not the predominant process explaining the decrease of $\mu^{182}W$

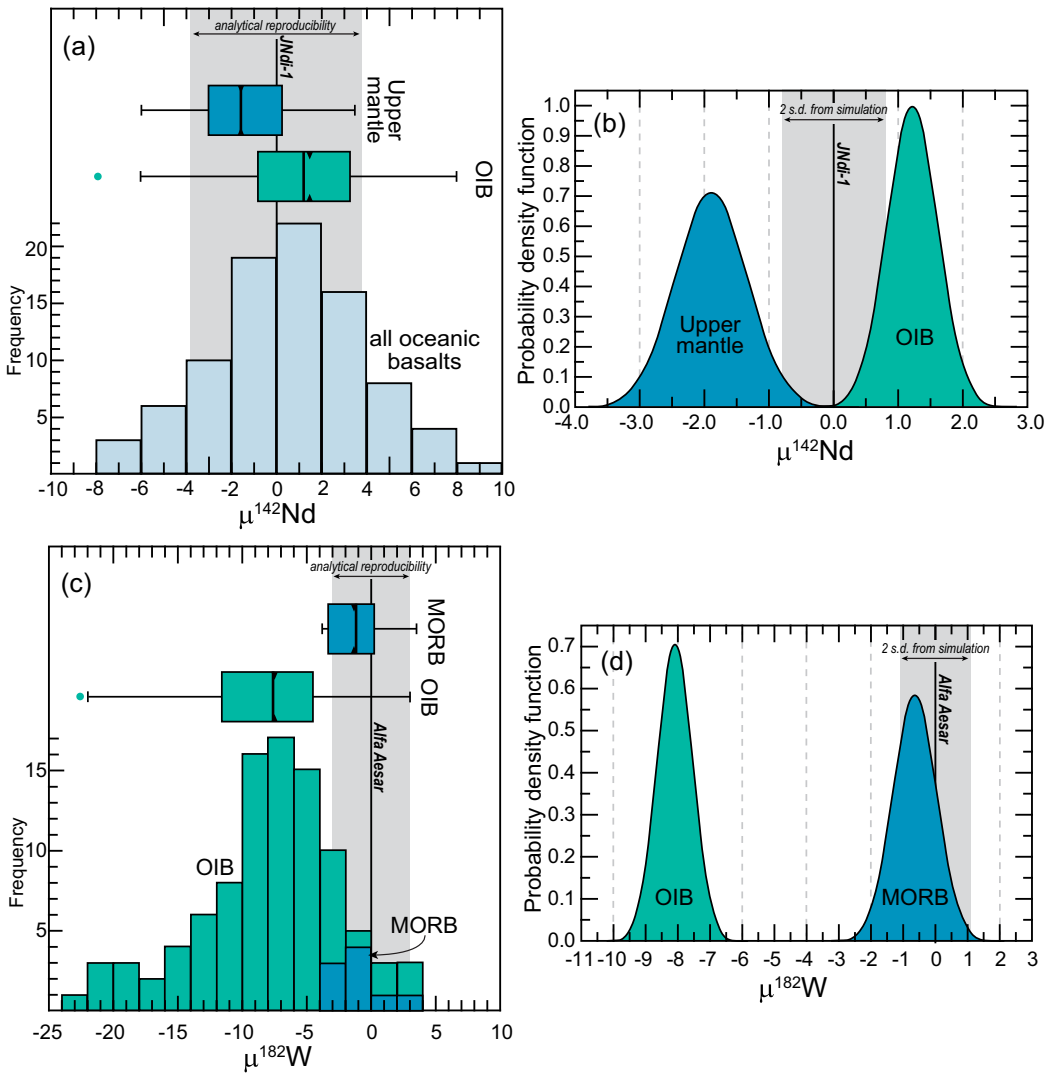

Figure 2 Compilation and computed probability density of **(a, b)** μ^{142}Nd and **(c, d)** μ^{182}W for MORB, OIB and mantle peridotites. Upper mantle **(a)** includes MORB and mantle peridotite samples. Left side plots **(a and c)** present histograms of all data; grey bands show the analytical reproducibility on the standards obtained during this study; thick bars on box plots present the median, and the triangle notches show the weighted mean values. Right side plots **(b, d)** show compositions generated by Monte Carlo bootstrap simulations (10,000 runs). Vertical lines and grey areas in **b and d** show the mean and 2 s.d. envelope of the Nd and W standards derived from the simulations. Database and references provided in the Supplementary Information Data Table S-4.

in the mantle. Furthermore, late accretion cannot explain μ^{182}W-He correlations found in some OIB (*e.g.*, Mundl *et al.*, 2017), since noble gas characteristics are most likely not preserved after impacts.

The model that would best explain the μ^{182}W observations, supported by a wide range of evidence such as seismology, multiple radiogenic isotope systems, and trace element geochemistry, is some mass transfer from mantle plumes into the upper mantle. Negative μ^{182}W in modern rocks is currently exclusively associated with plume-derived magmas, showing μ^{182}W values as low as −22.7 (Mundl *et al.*, 2017). Ocean island basalts, the lavas derived from mantle plumes, also display a range of Sr, Nd and Pb isotope compositions (*e.g.*, Zindler and Hart, 1986), believed to result from the incorporation of recycled components (sediments, crust) into the plume sources over time (*e.g.*, Hofmann and White, 1982). Although the μ^{182}W variability of the PAR MORB is only within 5 ppm, μ^{182}W values appear to be correlated with $(La/Gd)_N$ and Sr, Pb, and Nd isotopic compositions (Fig. 3a–d). For example, sample PAC2DR27-1, characterised as a Transitional-MORB (T-MORB), presents the lowest measured μ^{182}W and is the most trace element enriched basalt, with the most radiogenic $^{206}Pb/^{204}Pb$ and $^{87}Sr/^{86}Sr$ ratios, and the lowest $^{143}Nd/^{144}Nd$ (Fig. 3a–d, and Fig. S-2). The correlations between μ^{182}W *vs.* $(La/Gd)_N$ and Sr, Pb, and Nd isotopic compositions could be evidence of the progressive incorporation of mantle plume material into the upper mantle. Although the μ^{182}W variability observed in the PAR MORB is small, mantle melting averages the isotope heterogeneity present in the mantle sources (*e.g.*, Stracke, 2021), and thus the μ^{182}W variability shown in Figures 3a–d likely represent a minimum estimate for the total range of μ^{182}W variability of their mantle sources.

Different Causes for ^{142}W and ^{142}Nd Variability, but Shared Process for Their Decrease

The ultimate source of negative μ^{182}W in plume-derived magmas, and the 10–20 ppm μ^{182}W decrease from the Archean

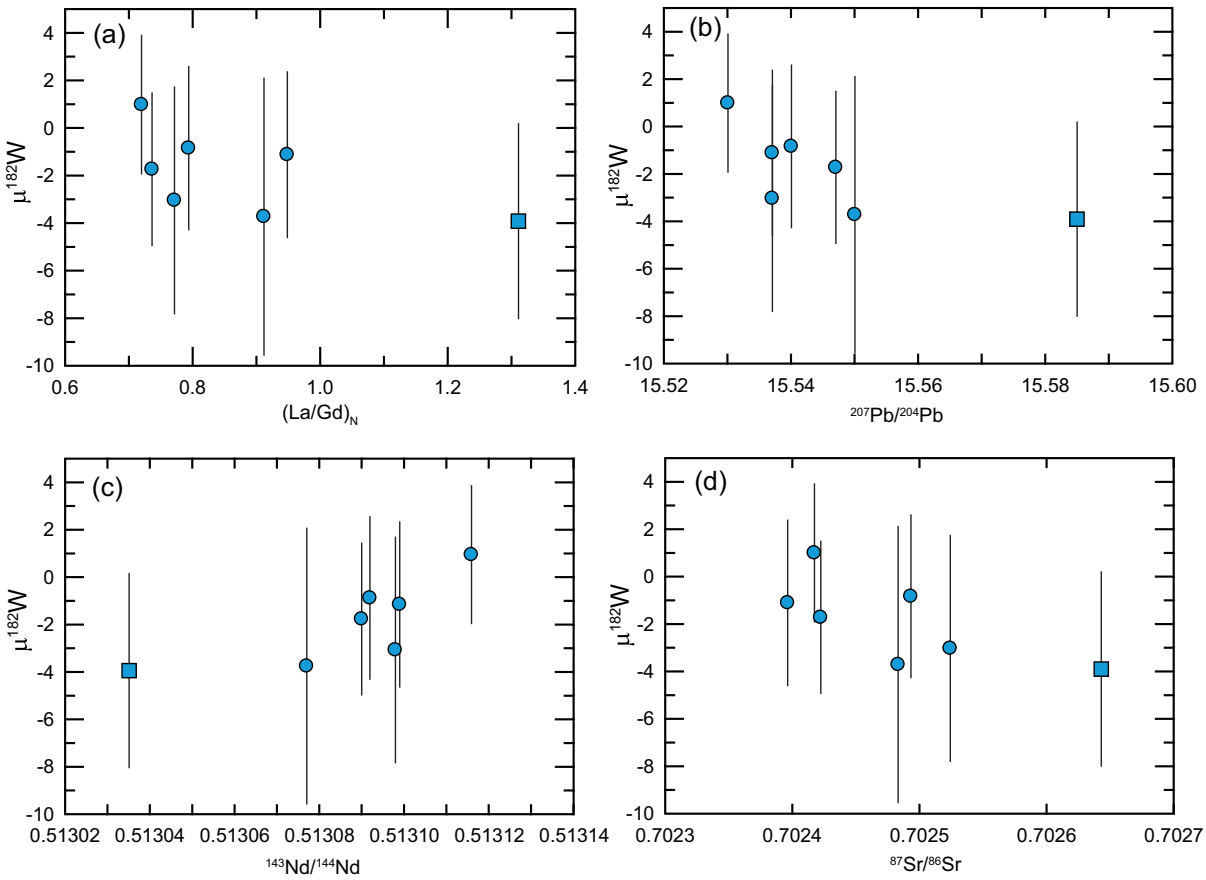

Figure 3 $\mu^{182}W$ *vs.* **(a)** normalised La/Gd ratio, and radiogenic **(b)** Pb, **(c)** Nd and **(d)** Sr isotope compositions, for the PAR MORB analysed here. Blue circles are N-MORB and square is T-MORB sample PAC2DR27-1. Tungsten isotope data from this study. Trace element concentrations and radiogenic isotope compositions from Hamelin *et al.* (2011).

to the modern mantle, has recently been the subject of active research. For example, chemical interaction between the core and the base of the mantle has been proposed to explain the negative $\mu^{182}W$ of plume-derived magmas (*e.g.*, Rizo *et al.*, 2019), given that the core is characterised by $\mu^{182}W$ of ~−200 and W concentration of ~0.5 ppm (*e.g.*, Kleine and Walker, 2017). While the decrease in $\mu^{182}W$ was found to require unrealistically high time-integrated plume flux or unrealistically low $\mu^{182}W$ in the plumes (Peters *et al.*, 2021), recent studies propose viable models for the $\mu^{182}W$ decline taking into account W diffusion from the core into the mantle and the residence time of W at the core-mantle boundary (Kaare-Rasmussen *et al.*, 2023).

The $\mu^{142}Nd$ difference between the DMM and OIB sources (Fig. 2) shows that these reservoirs could have separated ~4.45 Gyr ago, consistent with the I-Xe interpretation (Mukhopadhyay, 2012). The coupled low $\mu^{182}W$ and low $\mu^{142}Nd$ in some ~3.6 Ga komatiites could represent remanent fingerprints of this differentiation (Puchtel *et al.*, 2016). Most ^{182}W and ^{142}Nd comparative studies, however, imply different causes for the isotope variability in mantle-derived magmas. Nevertheless, shared underlying processes could have driven the decrease in magnitude of ^{182}W and ^{142}Nd variations. Given the available data, the period of $\mu^{182}W$ decrease between 3 and 2.4 Ga (Tusch *et al.*, 2021; Nakanishi *et al.*, 2023) seems to coincide with the timing of the homogenisation of $\mu^{142}Nd$ heterogeneities due to mantle mixing (*e.g.*, Carlson *et al.*, 2019). The onset of deep cold slab subduction in the early Earth (Klein *et al.*, 2017) might have generated upwellings from the core-mantle boundary, carrying negative $\mu^{182}W$, which gets remixed into the convective mantle. The number of combined ^{182}W and ^{142}Nd isotope studies in the same rock samples is limited. However, conducting similar additional investigations in Proterozoic rocks is crucial for enhancing our understanding of the timescales of mantle stirring and the geodynamic processes that have shaped Earth's modern mantle composition.

Acknowledgements

We acknowledge the generous support from the Carnegie Institution for Science Tuve Fellow Visiting Scientists program to H.R. and to J.O., allowing the writing of this manuscript. We thank Mike Walter, Peter van Keken and James W. Dottin III for helpful discussions, as well as the comments from Bradley Peters and an anonymous reviewer, which contributed to enhancing this manuscript. We are grateful to Pierre-Luc Lacroix for generating the code for the Monte Carlo bootstrap simulations. We thank the technical support provided by Shuangquan Zhang, Nimal DeSilva and Smita Mohanty at the IGGRC of Carleton University and the University of Ottawa Geochemistry Laboratory. This research was funded by the Natural Sciences and Engineering Research Council of Canada Discovery grant to H.R. (RGPIN-477144-2015) to J.O. (RGPIN 435589-2013), and the Ontario Early Researcher Award to H.R.

Editor: Helen Williams

Additional Information

Supplementary Information accompanies this letter at https://www.geochemicalperspectivesletters.org/article2412.

Cite this letter as: Peters, D., Rizo, H., O'Neil, J., Hamelin, C., Shirey, S.B. (2024) Comparative ^{142}Nd and ^{182}W study of MORBs and the 4.5 Gyr evolution of the upper mantle. *Geochem. Persp. Let.* 29, 51–56. https://doi.org/10.7185/geochemlet.2412

References

Boyet, M., Carlson, R.W. (2006) A new geochemical model for the Earth's mantle inferred from ^{146}Sm–^{142}Nd systematics. *Earth and Planetary Science Letters* 250, 254–268. https://doi.org/10.1016/j.epsl.2006.07.046

Carlson, R.W., Garçon, M., O'Neil, J., Reimink, J., Rizo, H. (2019) The nature of Earth's first crust. *Chemical Geology* 530, 119321. https://doi.org/10.1016/j.chemgeo.2019.119321

Caro, G., Bourdon, B., Birck, J.L., Moorbath, S. (2006) High-precision ^{142}Nd/^{144}Nd measurements in terrestrial rocks: constraints on the early differentiation of the Earth's mantle. *Geochimica et Cosmochimica Acta* 70, 164–191. https://doi.org/10.1016/j.gca.2005.08.015.

Cipriani, A., Bonatti, E., Carlson, R.W. (2011) Nonchondritic ^{142}Nd in suboceanic mantle peridotites. *Geochemistry, Geophysics, Geosystems* 12, Q03006. https://doi.org/10.1029/2010GC003415

Frossard, P., Israel, C., Bouvier, A., Boyet, M. (2022) Earth's composition was modified by collisional erosion. *Science* 377, 1529–1532. https://doi.org/10.1126/science.abq7351

Gale, A., Dalton, C.A., Langmuir, C.H., Su, Y., Schilling, J.G. (2013) The mean composition of ocean ridge basalts. *Geochemistry, Geophysics, Geosystems* 14, 489–518. https://doi.org/10.1029/2012GC004334

Hamelin, C., Dosso, L., Hanan, B.B., Moreira, M., Kositsky, A.P., Thomas, M.Y. (2011) Geochemical portray of the Pacific Ridge: New isotopic data and statistical techniques. *Earth and Planetary Science Letters* 302, 154–162. https://doi.org/10.1016/j.epsl.2010.12.007

Hofmann, A.W., White, W.M. (1982) Mantle plumes from ancient oceanic crust. *Earth and Planetary Science Letters* 57, 421–436. https://doi.org/10.1016/0012-821X(82)90161-3

Hyung, E., Jacobsen, S.B. (2020) The ^{142}Nd/^{144}Nd variations in mantle-derived rocks provide constraints on the stirring rate of the mantle from the Hadean to the present. *Proceedings of the National Academy of Sciences* 117, 14738–14744. https://doi.org/10.1073/pnas.2006950117

Jackson, M.G., Carlson, R.W. (2012) Homogeneous superchondritic ^{142}Nd/^{144}Nd in the mid-ocean ridge basalt and ocean island basalt mantle. *Geochemistry, Geophysics, Geosystems* 13, Q06011. https://doi.org/10.1029/2012GC004114

Johnston, S., Brandon, A., McLeod, C., Rankenburg, K., Becker, H., Copeland, P. (2022) Nd isotope variation between the Earth–Moon system and enstatite chondrites. *Nature* 611, 501–506. https://doi.org/10.1038/s41586-022-05265-0

Kaare-Rasmussen, J., Peters, D., Rizo, H., Carlson, R.W., Nielsen, S.G., Horton, F. (2023) Tungsten isotopes in Baffin Island lavas: Evidence of Iceland plume evolution. *Geochemical Perspectives Letters* 28, 7–12. https://doi.org/10.7185/geochemlet.2337

Klein, B.Z., Jagoutz, O., Behn, M.D. (2017) Archean crustal compositions promote full mantle convection. *Earth and Planetary Science Letters* 474, 516–526. https://doi.org/10.1016/j.epsl.2017.07.003

Kleine, T., Walker, R.J. (2017) Tungsten isotopes in planets. *Annual Review of Earth and Planetary Sciences* 45, 389–417. https://doi.org/10.1146/annurev-earth-063016-020037

König, S., Münker, C., Hohl, S., Paulick, H., Barth, A.R., Lagos, M., Pfänder, J., Büchl, A. (2011) The Earth's tungsten budget during mantle melting and crust formation. *Geochimica et Cosmochimica Acta 75,* 2119–2136. https://doi.org/10.1016/j.gca.2011.01.031

Mukhopadhyay, S. (2012) Early differentiation and volatile accretion recorded in deep-mantle neon and xenon. *Nature* 486, 101–104. https://doi.org/10.1038/nature11141

Mundl, A., Touboul, M., Jackson, M.G., Day, J.M.D., Kurz, M.D., Lekic, V., Helz, R.T., Walker, R.J. (2017) Tungsten-182 heterogeneity in modern ocean island basalts. *Science* 356, 66–69. https://doi.org/10.1126/science.aal4179

Mundl, A., Walker, R.J., Reimink, J.R., Rudnick, R.L., Gaschnig, R.M. (2018) Tungsten-182 in the upper continental crust: Evidence from glacial diamictites. *Chemical Geology* 494, 144–152. https://doi.org/10.1016/j.chemgeo.2018.07.036

Nakanishi, N., Puchtel, I.S., Walker, R.J., Nabelek, P.I. (2023) Dissipation of Tungsten-182 Anomalies in the Archean Upper Mantle: Evidence from the Black Hills, South Dakota, USA. *Chemical Geology* 617, 121255. https://doi.org/10.1016/j.chemgeo.2022.121255

Peters, B.J., Mundl-Petermeier, A., Carlson, R.W., Walker, R.J., Day, J.M.D. (2021) Combined Lithophile-Siderophile Isotopic Constraints on Hadean Processes Preserved in Ocean Island Basalt Sources. *Geochemistry, Geophysics, Geosystems* 22, 1–20. https://doi.org/10.1029/2020GC009479

Puchtel, I.S., Blichert-Toft, J., Touboul, M., Horan, M.F., Walker, R.J. (2016) The coupled ^{182}W-^{142}Nd record of early terrestrial mantle differentiation. *Geochemistry, Geophysics, Geosystems* 17, 2168–2193. https://doi.org/10.1002/2016GC006324

Rizo, H., Walker, R.J., Carlson, R.W., Horan, M.F., Mukhopadhyay, S., Manthos, V., Francis, D., Jackson, M.G. (2016) Preservation of Earth-forming events in the tungsten isotopic composition of modern flood basalts. *Science* 352, 809–812. https://doi.org/10.1126/science.aad8563

Rizo, H., Andrault, D., Bennett, N.R., Humayun, M., Brandon, A., Vlastelic, I., Moine, B., Poirier, A., Bouhifd, M.A., Murphy, D.T. (2019) ^{182}W evidence for core-mantle interaction in the source of mantle plumes. *Geochemical Perspectives Letters* 11, 6–11. https://doi.org/10.7185/geochemlet.1917

Stracke, A. (2021) A process-oriented approach to mantle geochemistry. *Chemical Geology* 579, 120350. https://doi.org/10.1016/j.chemgeo.2021.120350

Touboul, M., Puchtel, I.S., Walker, R.J. (2012) ^{182}W evidence for long-term preservation of early mantle differentiation products. *Science* 335, 1065–1069. https://doi.org/10.1126/science.1216351

Tucker, J.M., van Keken, P.E., Jones, R.E., Ballentine, C.J. (2020) A role for subducted oceanic crust in generating the depleted mid-ocean ridge basalt mantle. *Geochemistry, Geophysics, Geosystems* 21, e2020GC009148. https://doi.org/10.1029/2020GC009148

Tusch, J., Münker, C., Hasenstab, E., Jansen, M., Marien, C.S., Kurzweil, F., van Kranendonk, M.J., Smithies, H., Maier, W., Garbe-Schönberg, D. (2021) Convective isolation of hadean mantle reservoirs through archean time. *Proceedings of the National Academy of Sciences of the United States of America* 118, e2012626118. https://doi.org/10.1073/pnas.2012626118

Tusch, J., Hoffmann, J.E., Hasenstab, E., Fischer-Gödde, M., Marien, C.S., Wilson, A.H., Münker, C. (2022) Long-term preservation of Hadean protocrust in Earth's mantle. *Proceedings of the National Academy of Sciences* 119, e2120241119. https://doi.org/10.1073/pnas.2120241119

Willbold, M., Elliott, T., Moorbath, S. (2011) The tungsten isotopic composition of the Earth's mantle before the terminal bombardment. *Nature* 477, 195–198. https://doi.org/10.1038/nature10399

Zindler, A., Hart, S. (1986) Chemical geodynamics. *Annual Review of Earth and Planetary Sciences* 14, 493–571. https://doi.org/10.1146/annurev.ea.14.050186.002425

Geochemical Perspectives Letters

Comparative ^{142}Nd and ^{182}W study of mid-ocean ridge basalts and the 4.5 Gyr evolution of the upper mantle

D. Peters, H. Rizo, J. O'Neil, C. Hamelin, S.B. Shirey

Supplementary Information

The Supplementary Information includes:

- Sample Description
- Methods
- Figures S-1 to S-4
- Data Tables S-1 to S-4
- Supplementary Information References

Sample Description

The mid-ocean ridge basalts studied here were sampled during the PACANTARCTIC2 cruise (2004-2005) along the Pacific Antarctic Ridge (PAR) between 53°S and 41°S (**Fig. S-1**). The goal of the PACANTARTIC2 cruise was to sample the ridge furthest away possible from any hotspot, in order to study the composition of the depleted upper mantle. The morphology (median values of the ridge axis bathymetry and ridge cross-section) of the ridge sampled during the PACANTARCTIC2 is consistent with a normal fast spreading ridge (*e.g.*, Briais *et al.*, 2009), which differs from a hotspot-ridge interaction setting. The closest hotspot-ridge interaction from the studied PAR area is the Foundation hotspot ~800 km north, and the 2nd closest is the Louisville hotspot ~1200 km south. The PAR is a fast-spreading context where along axis fluxes are limited, and thus hotspot contributions are negligible over such long distances. The lack of hotspot influence in the samples studied is further supported by geochemical studies (*e.g.*, Moreira *et al.*, 2008; Hamelin *et al.*, 2010, 2011; Labidi *et al.*, 2014; Bezard *et al.*, 2016). Trace element ratios, such as $(La/Sm)_N$ are within the domain of 'normal MORB' (Hamelin *et al.*, 2010). Geochemical compositions in Sr-Nd-Pb-Hf of these samples can be found in Hamelin *et al.* (2011) and plot close to the DMM end member. The range of radiogenic compositions in that study are attributed to the partial melting of a « marble-cake » mantle assemblage, unrelated to plume-ridge interactions. Additionally, helium isotopes of the Pacific-Antarctic Ridge between 41.5 and 52.5° S show a lack of hotspot influence along that section of the ridge (Moreira *et al.*, 2008).

Tungsten concentrations in the PAR MORBs studied here (n = 18) vary from 6.8 ng g^{-1} to 220 ng g^{-1} (**Data Table S-1**). The W concentrations are strongly coupled to other immobile and incompatible trace elements such as Nb and Th, and W/Th ratios are within the range of fresh MORB (**Fig. S-2**). This implies that W contained in the MORB samples studied is derived from their mantle sources (*e.g.*, König *et al.*, 2011) and free from secondary W overprinting.

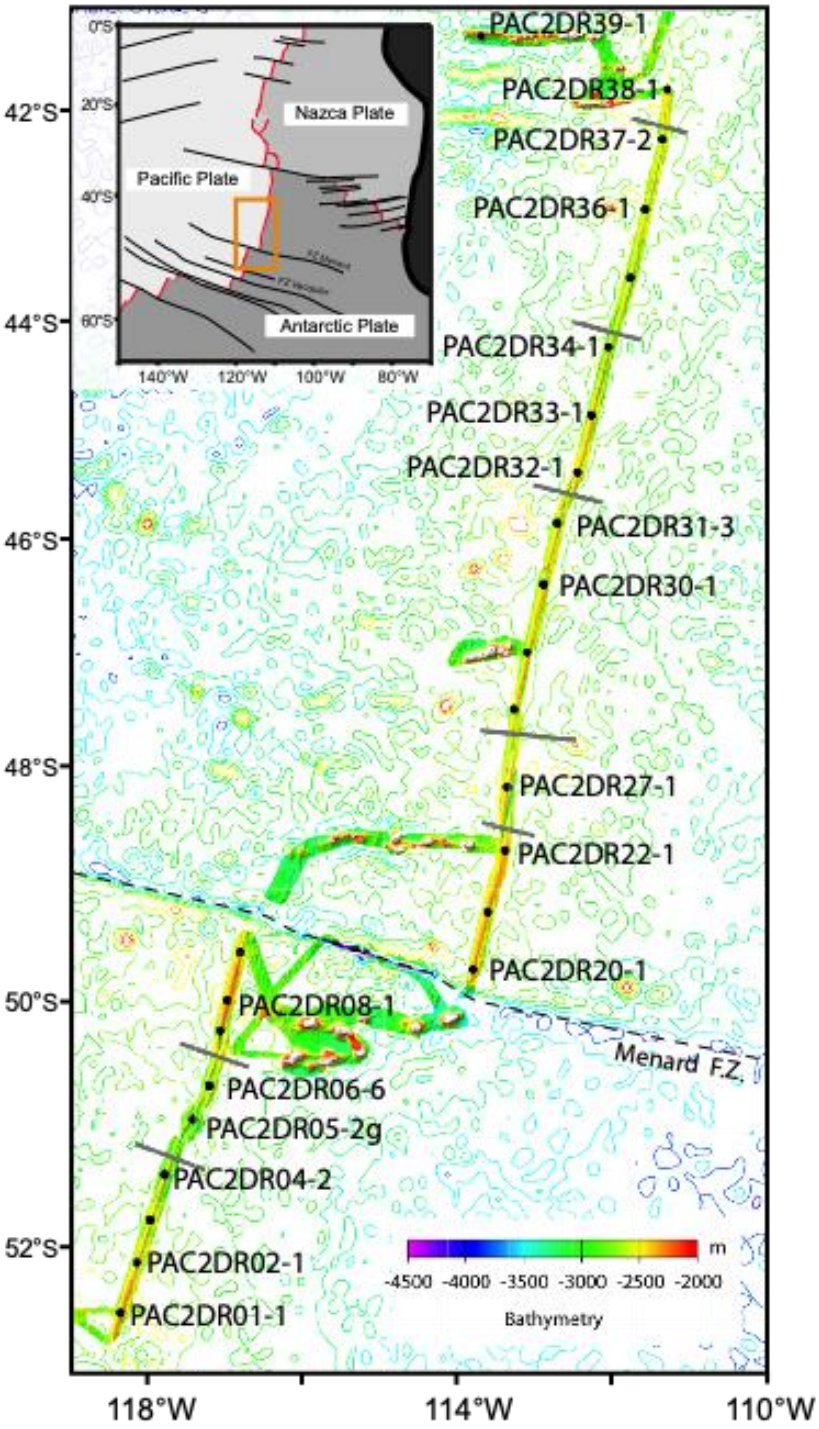

Figure S-1 Map of the Pacific-Antarctic Ridge. Black dots are dredged samples during the PACANTARCTIC2 cruise. Grey lines are overlapping spreading centres (OSC) bordering second order segmentation of the ridge axis.

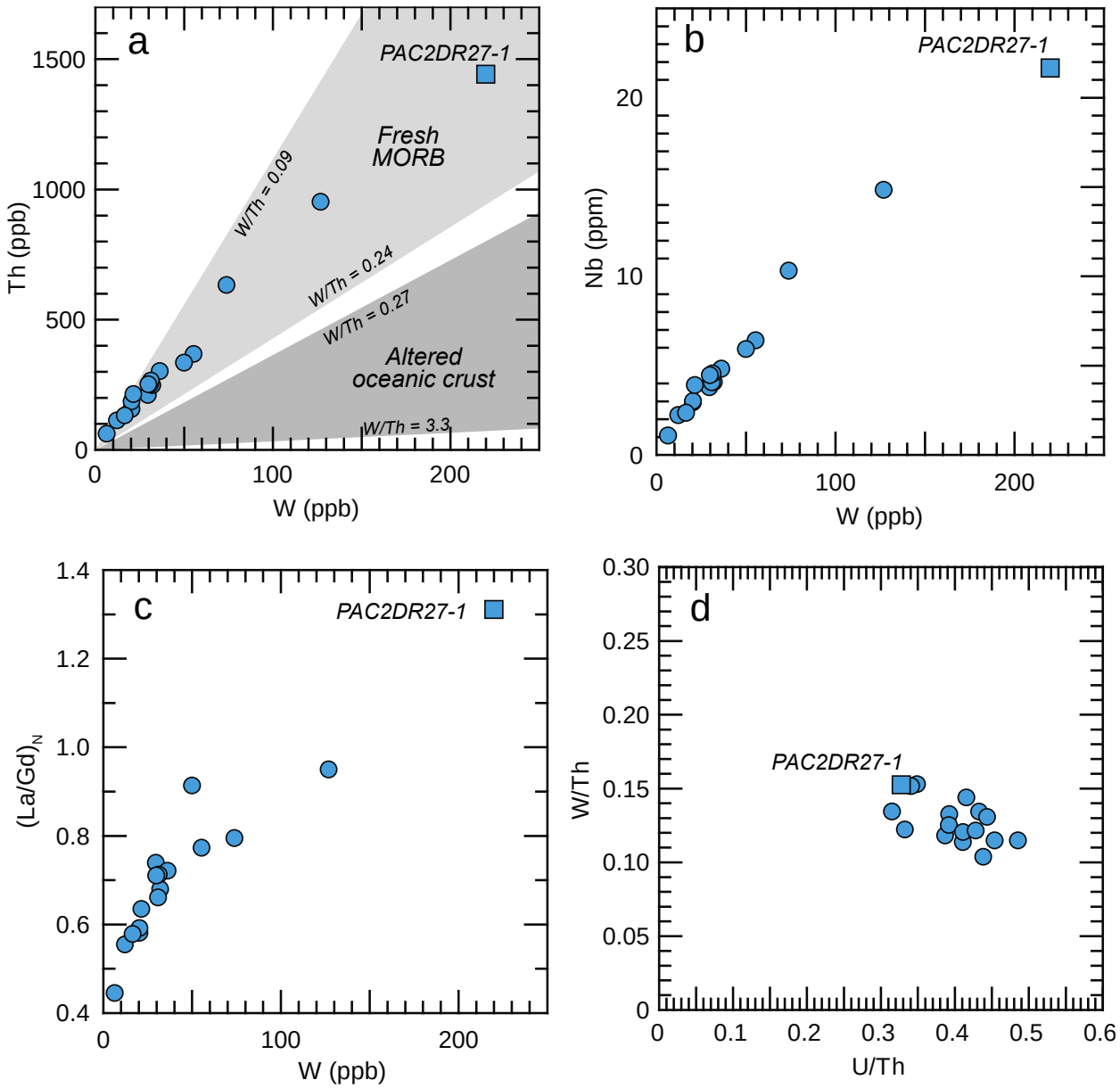

Figure S-2 Tungsten vs. other highly incompatible trace element concentrations and the normalized La/Gd ratio of the Pacific-Atlantic ridge basalts. Tungsten concentrations from this study, other trace element concentrations from Hamelin *et al.* (2010), Labidi *et al.* (2014) and Yierpan *et al.* (2019). Fresh MORB W/Th ranges from König *et al.* (2011), altered oceanic crust W/Th ranges from Reifenröther *et al.* (2021).

Methods

Tungsten concentration analysis

Tungsten concentrations (**Data Table S-1**) were determined by isotope dilution using a ^{186}W spike. Approximately 0.1 g of sample powder was dissolved in a mixture of 4 mL 29 M HF and 1 mL 15 M HNO_3,

followed by repeated dissolutions in 1 mL 6N HCl. Samples were spiked at the onset of digestion to insure sample-spike equilibration. Tungsten was isolated using ion chromatography techniques similar to the ones described in Nagai and Yokoyama (2014). Isotope ratio measurements were carried out on a ThermoScientific Neptune MC-ICPMS of the Isotope Geochemistry and Geochronology Research Centre (IGGRC) of Carleton University (Ottawa, Canada). Measurements were performed on 1.5 ppb W 0.5 M HNO_3 + 0.05 HF solutions. Two standard deviation measurement precisions are largely 2-4 %, propagated 2 standard deviations are estimated better than 10 % in most cases (largely by uncertainty of the spike concentration). Monitoring the measurement accuracy of isotope dilution concentration analysis with the USGS basalt standards BHVO-2 and BCR-2 yielded 193 ± 18 ng g^{-1} and 436 ± 47 ng g^{-1}, respectively, which are similar within errors of previously reported concentrations (*e.g.*, Jochum *et al.*, 2016; Kurzweil *et al.*, 2018). Total chemistry blanks were 260 pg, representing 1-2 % of the W analysed in samples.

Tungsten isotope analysis

High precision W isotope compositions (**Data Table S-2**) were also obtained at the IGGRC of Carleton University. Sample masses between 3.4 g and 24.5 g were dissolved and W was separated following similar methods described in Touboul and Walker (2012) and Breton and Quitté (2014). Tungsten separation for isotope analysis was performed using a first 20 mL AG50W-X8 resin (200-400 mesh) column to remove matrix elements, and a second 10 mL AG1-X8 resin (200–400 mesh) column to separate W from other high field strength elements (HFSE). Purified W solutions were passed through an additional AG1-X8 resin (200–400 mesh) micro-column (0.3 mL) mainly to remove Ti traces that could reduce the ionization efficiency of W. Tungsten yields were 50-70 %, procedural blanks ranged between 0.4 to 3.0 ng, respectively, for ~ 440 to 530 ng of W separates representing less than 1 % of the total W.

Tungsten isotope ratios were measured on a ThermoScientific Triton TIMS, using the setup and protocols described in Archer *et al.* (2017) and Rizo *et al.* (2019). Results were interference-corrected using the oxygen isotope compositional relations from Archer *et al.* (2017) and mass bias-corrected by internal normalisation to $^{186}W/^{184}W = 0.92767$ (Völkening *et al.*, 1991) (normalisation to $^{186}W/^{183}W = 1.985936$ was also performed and results shown in **Data Table S-2**). The $^{182}W/^{184}W$ and $^{183}W/^{184}W$ ratios are reported as μ notations, which are deviations in parts per million (ppm) from the isotope composition of the Alfa Aesar W standard. This standard yielded $^{182}W/^{184}W = 0.864888 \pm 0.000003$ (2 s.d.; n = 6), and $^{183}W/^{184}W = 0.467149 \pm 0.000001$ (2 s.d.; n = 7). Two additional measurements of the NIST standard 3163 yielded mean $\mu^{182}W = 2.4 \pm 6.0$ (2 s.d.) and $\mu^{183}W = -1.4 \pm 2.9$ (2 s.d.). No residual mass-dependent fractionation is observed in the dataset (**Fig. S-3**). The $\mu^{182}W$ errors of means are ± 2σ standard deviations (2 s.d.) of the sample populations, or 2σ standard errors (2 s.e.) of the individual measurements.

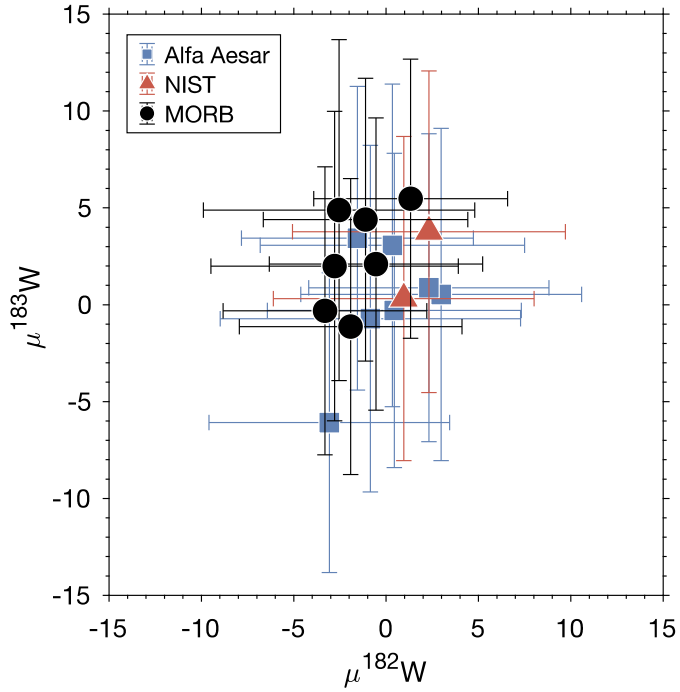

Figure S-3 $\mu^{183}W$ vs $\mu^{182}W$ of the MORB samples of this study, as well as of the Alfa Aesar W standard and the W isotope standard reference material 3163 from the National the Institute of Standards and Technology (NIST). Both $\mu^{183}W$ vs $\mu^{182}W$ shown are mass bias-corrected using $^{186}W/^{184}W$.

Neodymium isotope analysis

Fourteen MORB samples have been analysed for high-precision Nd isotopic compositions (**Data Table S-3**). Chemical separation and purification of Nd were performed at the Advanced Research Complex of University of Ottawa, Canada, following the protocols of Garçon *et al.* (2018) and Li *et al.* (2015), and only the main steps are summarized here. The light-REE were separated from the whole-rock matrix using 200-400 mesh AG50W-X8 cation-exchange resin. The dried light-REE fractions were dissolved in HNO_3 with $NaBrO_3$ to oxidize Ce to its +4 form and remove it from other light-REE+3 using columns filled with 100-150 µm Eichrom LnSpec resin. The Na and Br added during the Ce-removal procedure were then removed using AG50W-X8 cation-exchange resin. The Nd was finally purified from Sm and any remaining Ce using thin columns filled with 20-50 µm Eichrom LnSpec resin. Total chemistry Nd yields were ≥ 90 %, the total procedural Nd blank was 16 pg.

High-precision Nd isotope abundance ratio measurements were performed on a ThermoScientific Triton TIMS at the Isotope Geochemistry and Geochronology Research Centre of Carleton University (Ottawa, Canada). Samples were loaded onto zone-refined 99.999 % Re filaments and Nd isotopes were measured on double filaments and using a 2-step dynamic routine that provided static measurements of all Nd abundance isotope ratios and dynamic measurements of the $^{142}Nd/^{144}Nd$ ratio. The mass/charge ratios 140^+ and 147^+ were monitored for Ce and Sm mass interference corrections. Each run consisted of 600 to 1200 ratios measured in blocks of 25 cycles, with an integration time of 8.39 seconds per step and a background measurement of 30s between each block. Data were corrected for instrumental mass fractionation using the exponential law to $^{146}Nd/^{144}Nd = 0.7219$. Samples were measured at the same time as the JNdi-1 Nd standard, and in two

analytical sessions (Session 1 and Session 2; **Data Table S-3**). For Session 1, repeated measurement of the JNdi-1 standard yielded an average $^{142}Nd/^{144}Nd = 1.141835 \pm 0.000004$ (2 s.d., n = 14), corresponding to a repeatability of 3.8 ppm. For Session 2, the JNdi-1 yielded an average $^{142}Nd/^{144}Nd = 1.141836 \pm 0.000004$ (2 s.d., n = 6), corresponding to a repeatability of 3.3 ppm. The average $^{143}Nd/^{144}Nd$ ratio for the JNdi-1 standard for both sessions was 0.512107 ± 0.000003 (2 s.d.), and within error of the value of Tanaka *et al.* (2000) of 0.512115 ± 0.000007. The $\mu^{142}Nd$ errors of means are ± 2σ standards deviations (2 s.d.) of the sample populations or 2σ standard errors (2 s.e.) of the individual measurements.

The $\mu^{142}Nd$ obtained for the PAR MORB samples do not correlate with their $\mu^{182}W$ (**Fig. S-4**).

A database for all available $\mu^{142}Nd$ for MORB, OIB and mantle peridotites is provided in the **Data Table S-4**.

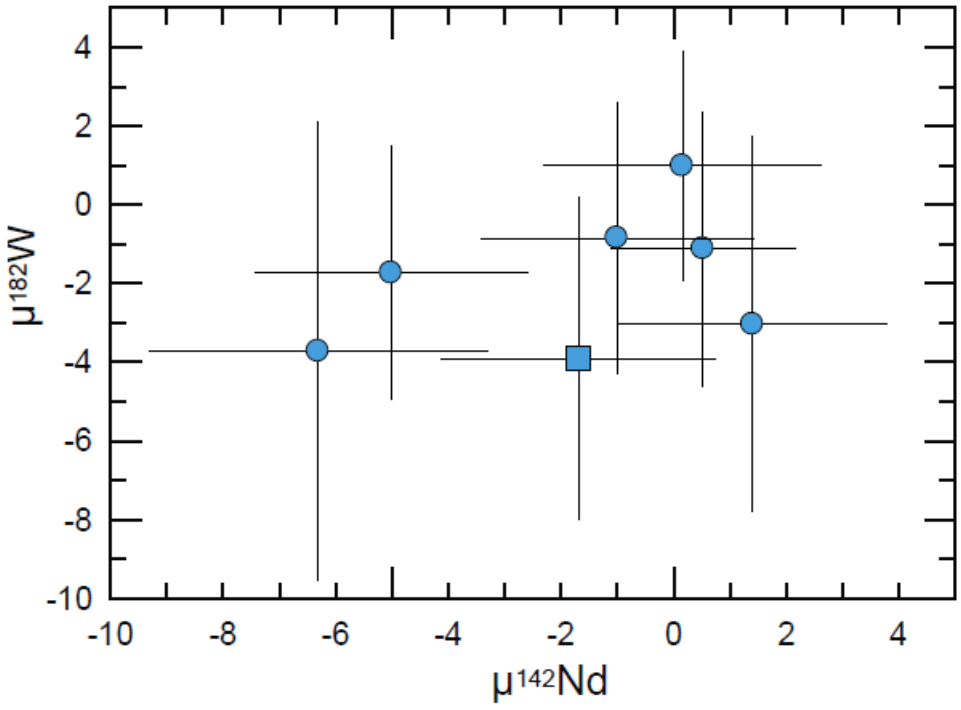

Figure S-4 $\mu^{182}W$ *vs.* $\mu^{142}Nd$ of the PAR MORB samples of this study. Errors shown are ± 2 s.e. Square symbol for sample PAC2DR27-1 (T-MORB).

Supplementary Information Data Tables

Data Tables S-1 to S-4 (Excel) can be downloaded from the online version of this article at https://doi.org/10.7185/geochemlet.2412.

Data Table S-1 Tungsten abundances for the PAR MORB samples of this study, and the USGS rock reference materials BHVO-2 and BCR-2.

Data Table S-2 Detailed high-precision W isotope measurements for the PAR MORB samples of this study. Tungsten isotope ratios normalised to $^{186}W/^{184}W$ (spreadsheet 1), or $^{186}W/^{183}W$ (spreadsheet 2).

Data Table S-3 Detailed high-precision Nd isotope measurements for the PAR MORB samples of this study.

Data Table S-4 Compilation of published $\mu^{142}Nd$ and $\mu^{182}W$ for MORB, OIB and mantle peridotites.

Supplementary Information References

Andreasen, R., Sharma, M., Subbarao, K.V., Viladkar, S.G. (2008) Where on Earth is the enriched Hadean reservoir?. *Earth and Planetary Science Letters* 266, 14-28. https://doi.org/10.1016/j.epsl.2007.10.009

Archer, G. J., Mundl, A., Walker, R.J., Worsham, E.A., Bermingham, K.R. (2017) High-precision analysis of $^{182}W/^{184}W$ and $^{183}W/^{184}W$ by negative thermal ionization mass spectrometry: Per-integration oxide corrections using measured $^{18}O/^{16}O$. *International Journal of Mass Spectrometry* 414, 80–86. https://doi.org/10.1016/j.ijms.2017.01.002

Bezard, R., Fischer-Gödde, M., Hamelin, C., Brennecka, G.A., Kleine, T. (2016) The effects of magmatic processes and crustal recycling on the molybdenum stable isotopic composition of Mid-Ocean Ridge Basalts. *Earth and Planetary Science Letters* 453, 171-181. https://doi.org/10.1016/j.epsl.2016.07.056

Boyet, M., Carlson, R.W. (2006) A new geochemical model for the Earth's mantle inferred from 146Sm–142Nd systematics. *Earth and Planetary Science Letters* 250, 254-268. https://doi.org/10.1016/j.epsl.2006.07.046

Breton, T., Quitté, G. (2014) High-precision measurements of tungsten stable isotopes and application to Earth sciences. *Journal of Analytical Atomic Spectrometry* 29, 2284-2293.https://doi.org/10.1039/C4JA00184

Briais, A., Ondreas, H., Klingelhoefer, F., Dosso, L., Hamelin, C., Guillou, H. (2009) Origin of volcanism on the flanks of the Pacific - Antarctic ridge between 41 ° 30' S and 52° S. *Geochemistry, Geophysics, Geosystems* 10, 9. https://doi.org/10.1029/2008GC002350

Caro, G., Bourdon, B., Birck, J.L., Moorbath, S. (2006) High-precision $^{142}Nd/^{144}Nd$ measurements in terrestrial rocks: constraints on the early differentiation of the Earth's mantle. *Geochimica et Cosmochimica Acta* 70, 164-191. https://doi.org/10.1016/j.gca.2005.08.015

Cipriani, A., Bonatti, E., Carlson, R.W. (2011) Nonchondritic 142Nd in suboceanic mantle peridotites. *Geochemistry, Geophysics, Geosystems* 12. https://doi.org/10.1029/2010GC003415

Garçon, M., Boyet, M., Carlson, R.W., Horan, M.F., Auclair, D., Mock, T.D. (2018) Factors influencing the precision and accuracy of Nd isotope measurements by thermal ionization mass spectrometry. *Chemical Geology* 476, 493-514. https://doi.org/10.1016/j.chemgeo.2017.12.003

Hamelin, C., Dosso, L., Hanan, B., Barrat, J.A., Ondréas, H. (2010) Sr - Nd - Hf isotopes along the Pacific Antarctic Ridge from 41 to 53° S. *Geophysical Research Letters* 37, 10.

Hamelin, C., Dosso, L., Hanan, B.B., Moreira, M., Kositsky, A.P., Thomas, M.Y. (2011) Geochemical portray of the Pacific Ridge: New isotopic data and statistical techniques. *Earth and Planetary Science Letters* 302, 154-162. https://doi.org/10.1016/j.epsl.2010.12.007

Horan, M.F., Carlson, R.W., Walker, R.J., Jackson, M., Garçon, M., Norman, M. (2018) Tracking Hadean processes in modern basalts with 142-Neodymium. *Earth and Planetary Science Letters*, 484, 184-191.https://doi.org/10.1016/j.epsl.2017.12.017

Hyung, E., Jacobsen, S.B. (2020) The 142Nd/144Nd variations in mantle-derived rocks provide constraints on the stirring rate of the mantle from the Hadean to the present. *Proceedings of the National Academy of Sciences*, 117, 14738-14744. https://doi.org/10.1073/pnas.2006950117

Jackson, M.G., Carlson, R.W. (2012) Homogeneous superchondritic $^{142}Nd/^{144}Nd$ in the mid - ocean ridge basalt and ocean island basalt mantle. *Geochemistry, Geophysics, Geosystems* 13. https://doi.org/10.1029/2012GC004114

Jackson, M.G., Blichert-Toft, J., Halldórsson, S.A., Mundl-Petermeier, A., Bizimis, M., Kurz, M.D., Price, A.A., Harðardóttir, S., Willhite, L.N., Breddam, K., Becker, T.W., Fischer, R.A. (2020) Ancient helium and tungsten isotopic signatures preserved in mantle domains least modified by crustal recycling. *Proceedings of the National Academy of Sciences*, 117, 30993-31001. https://doi.org/10.1073/pnas.2009663117

Jochum, K.P., Weis, U., Schwager, B., Stoll, B., Wilson, S.A., Haug, G.H., Andreae, M.O., Enzweiler, J. (2016) Reference values following ISO guidelines for frequently requested rock reference materials. *Geostandards and Geoanalytical Research* 40, 333-350. https://doi.org/10.1111/j.1751-908X.2015.00392.x

König, S., Münker, C., Hohl, S., Paulick, H., Barth, A.R., Lagos, M., Pfänder, J., Büchl, A. (2011) The Earth's tungsten budget during mantle melting and crust formation. *Geochimica et Cosmochimica Acta* 75, 2119-2136. https://doi.org/10.1016/j.gca.2011.01.031

Kruijer, T.S., Kleine, T. (2018) No 182W excess in the Ontong Java Plateau source. *Chemical Geology* 485, 24-31. https://doi.org/10.1016/j.chemgeo.2018.03.024

Kurzweil, F., Münker, C., Tusch, J., Schoenberg, R. (2018) Accurate stable tungsten isotope measurements of natural samples using a 180W-183W double-spike. *Chemical Geology* 476, 407-417. https://doi.org/10.1016/j.chemgeo.2017.11.037

Labidi, J., Cartigny, P., Hamelin, C., Moreira, M., Dosso, L. (2014) Sulfur isotope budget (32S, 33S, 34S and 36S) in Pacific–Antarctic ridge basalts: A record of mantle source heterogeneity and hydrothermal sulfide assimilation. *Geochimica et Cosmochimica Acta* 133, 47-67. https://doi.org/10.1016/j.gca.2014.02.023

Li, C.F., Wang, X.C., Li, Y.L., Chu, Z.Y., Guo, J.H., Li, X.H. (2015) Ce–Nd separation by solid-phase micro-extraction and its application to high-precision $^{142}Nd/^{144}Nd$ measurements using TIMS in geological materials. *Journal of Analytical Atomic Spectrometry* 30, 895-902. https://doi.org/10.1039/C4JA00328D

Mei, Q.F., Yang, J.H., Yang, Y.H. (2018) An improved extraction chromatographic purification of tungsten from a silicate matrix for high precision isotopic measurements using MC-ICPMS. *Journal of Analytical Atomic Spectrometry* 33, 569-577. https://doi.org/10.1039/C8JA00024G

Moreira, M.A., Dosso, L., Ondréas, H. (2008) Helium isotopes on the Pacific - Antarctic ridge (52.5°–41.5°S). *Geophysical Research Letters* 35, 10. https://doi.org/10.1029/2008GL033286

Mundl, A., Touboul, M., Jackson, M.G., Day, J.M.D., Kurz, M.D., Lekic, V., Helz, R.T., Walker, R.J. (2017) Tungsten-182 heterogeneity in modern ocean island basalts. *Science* 356, 66–69. https://doi.org/10.1126/science.aal4179

Mundl-Petermeier, A., Walker, R.J., Jackson, M.G., Blichert-Toft, J., Kurz, M.D., Halldórsson, S.A. (2019) Temporal evolution of primordial tungsten-182 and $^{3}He/^{4}He$ signatures in the Iceland mantle plume. *Chemical Geology* 525, 245–259. https://doi.org/10.1016/j.chemgeo.2019.07.026

Mundl-Petermeier, A., Walker, R.J., Fischer, R.A., Lekic, V., Jackson, M G., Kurz, M D. (2020) Anomalous 182W in high 3He/4He ocean island basalts: Fingerprints of Earth's core? *Geochimica et Cosmochimica Acta* 271, 194–211. https://doi.org/10.1016/j.gca.2019.12.020

Murphy, D.T., Brandon, A.D., Debaille, V., Burgess, R., Ballentine, C. (2010) In search of a hidden long-term isolated sub-chondritic $^{142}Nd/^{144}Nd$ reservoir in the deep mantle: Implications for the Nd isotope systematics of the Earth. *Geochimica et Cosmochimica Acta* 74, 738-750. https://doi.org/10.1016/j.gca.2009.10.005

Nagai, Y., Yokoyama, T. (2014) Chemical separation of Mo and W from terrestrial and extraterrestrial samples via anion exchange chromatography. *Analytical Chemistry* 86, 4856–48630. https://doi.org/10.1021/ac404223t

Peters, B.J., Mundl-Petermeier, A., Carlson, R.W., Walker, R.J., Day, J.M.D. (2021) Combined Lithophile-Siderophile Isotopic Constraints on Hadean Processes Preserved in Ocean Island Basalt Sources. *Geochemistry, Geophysics, Geosystems* 22, 1–20. https://doi.org/10.1029/2020GC009479

Peters, B.J., Carlson, R.W., Day, J.M. Horan, M.F. (2018) Hadean silicate differentiation preserved by anomalous 142Nd/144Nd ratios in the Réunion hotspot source. *Nature* 555, 89-93. https://doi.org/10.1038/nature25754

Reifenröther, R., Münker, C., Scheibner, B. (2021) Evidence for tungsten mobility during oceanic crust alteration. *Chemical Geology* 584, 120504. https://doi.org/10.1016/j.chemgeo.2021.120504

Rizo, H., Walker, R.J., Carlson, R.W., Horan, M.F., Mukhopadhyay, S., Manthos, V., Francis, D., Jackson, M.G. (2016) Preservation of Earth-forming events in the tungsten isotopic composition of modern flood basalts. *Science* 352, 809-812. https://doi.org/10.1126/science.aad8563

Rizo, H., Andrault, D., Bennett, N. R., Humayun, M., Brandon, A., Vlastélic, I., Moine, B., Poirier, A., Bouhifd, M.A., Murphy, D.

T. (2019) ^{182}W evidence for core-mantle interaction in the source of mantle plumes. *Geochemical Perspectives Letters* 11, 6-11.https://doi.org/10.7185/geochemlet.1917

Tanaka, T., Togashi, S., Kamioka, H., Amakawa, H., Kagami, H., Hamamoto, T., Yuhara, M., Orihashi, Y., Yoneda, S., Shimizu, H., Kunimaru, T. (2000) JNdi-1: a neodymium isotopic reference in consistency with LaJolla neodymium. *Chemical Geology* 168, 279-281. https://doi.org/10.1016/S0009-2541(00)00198-4

Touboul, M., Walker, R.J. (2012) High precision tungsten isotope measurement by thermal ionization mass spectrometry. *International Journal of Mass Spectrometry* 309, 109-117. https://doi.org/10.1016/j.ijms.2011.08.033

Völkening, J., Köppe, M., Heumann, K.G. (1991) Tungsten isotope ratio determinations by negative thermal ionization mass spectrometry. *International Journal of Mass Spectrometry and Ion Processes* 107, 361-368. https://doi.org/10.1016/0168-1176(91)80070-4

Yierpan, A., König, S., Labidi, J., Schoenberg, R. (2019) Selenium isotope and S-Se-Te elemental systematics along the Pacific-Antarctic ridge: Role of mantle processes. *Geochimica et Cosmochimica Acta* 249, 199-224. https://doi.org/10.1016/j.gca.2019.01.028